AN APPLICATION OF THE QUADRATURE-FREE DISCONTINUOUS GALERKIN METHOD

DAVID P. LOCKARD* AND HAROLD L. ATKINS†
NASA Langley Research Center, Hampton, VA 23681-2199, U.S.A

Introduction

The process of generating a block-structured mesh with the smoothness required for high-accuracy schemes is still a time-consuming process often measured in weeks or months. Unstructured grids about complex geometries are more easily generated, and for this reason, methods using unstructured grids have gained favor for aerodynamic analyses. The discontinuous Galerkin (DG) method is a compact finite-element projection method that provides a practical framework for the development of a high-order method using unstructured grids. Higher-order accuracy is obtained by representing the solution as a high-degree polynomial whose time evolution is governed by a local Galerkin projection. The traditional implementation of the discontinuous Galerkin uses quadrature for the evaluation of the integral projections and is prohibitively expensive. Atkins and Shu[1] introduced the quadrature-free formulation in which the integrals are evaluated a-priori and exactly for a similarity element. The approach has been demonstrated to possess the accuracy required for acoustics even in cases where the grid is not smooth. Other issues such as boundary conditions and the treatment of non-linear fluxes have also been studied in earlier work[2,3].

This paper describes the application of the quadrature-free discontinuous Galerkin method to a two-dimensional shear layer problem. First, a brief description of the method is given. Next, the problem is described and the solution is presented. Finally, the resources required to perform the calculations are given.

Numerical Method

The discontinuous Galerkin method is applicable to systems of first-order equations of the form

$$\frac{\partial \mathbf{q}}{\partial t} + \frac{\partial \mathbf{f}_i}{\partial x_i} = \mathbf{s}. \tag{1}$$

A summation convention is used for all repeated indices. Here, i ranges from unity to the number of coordinate directions. The domain of interest is divided into non-overlapping elements each of which is defined on some domain Ω with a boundary $\partial\Omega$. For the two-dimensional linearized Euler equations, $\mathbf{q}$, $\mathbf{f}$, and $\mathbf{s}$ are given by

$$\mathbf{q} = \begin{pmatrix} \rho \\ p \\ u \\ v \end{pmatrix}, \quad \mathbf{f}_1 = \begin{pmatrix} \overline{U} & 0 & \overline{\rho} & 0 \\ 0 & \overline{U} & \gamma\overline{P} & 0 \\ 0 & 1/\overline{\rho} & \overline{U} & 0 \\ 0 & 0 & 0 & \overline{U} \end{pmatrix}\mathbf{q}, \quad \mathbf{f}_2 = \begin{pmatrix} \overline{V} & 0 & 0 & \overline{\rho} \\ 0 & \overline{V} & 0 & \gamma\overline{P} \\ 0 & 0 & \overline{V} & 0 \\ 0 & 1/\overline{\rho} & 0 & \overline{V} \end{pmatrix}\mathbf{q},$$

*Research Scientist
†Senior Research Scientist

$$
\mathbf{s} \;=\; \begin{pmatrix} 0 & 0 & 0 & 0 \\ 0 & (1-\gamma)(\overline{U}_x + \overline{V}_y) & (\gamma-1)\overline{P}_x & (\gamma-1)\overline{P}_y \\ -(\overline{UU}_x + \overline{VU}_y)/\overline{\rho} & (1/\overline{\rho})_x & \overline{V}_y & -\overline{U}_y \\ -(\overline{UV}_x + \overline{VV}_y)/\overline{\rho} & (1/\overline{\rho})_y & -\overline{V}_x & \overline{U}_x \end{pmatrix} \mathbf{q}. \tag{2}
$$

The vector of dependent variables is $\mathbf{q}$. An over-line has been used to denote local temporal-mean quantities, and subscripted values denote differentiation. ρ and p are the perturbation density and pressure, and u and v are the x and y directed velocities, respectively. The ratio of specific heats is γ. The equations have been made dimensionless using the ambient speed of sound c_o as the reference velocity.

The discontinuous Galerkin method is obtained by approximating the solution in each element Ω in terms of an appropriate set of basis functions b_m.

$$
\mathbf{q} \approx \sum_{m=1}^{N} \boldsymbol{q}_m b_m = \boldsymbol{q}_m b_m
$$

where $\{b_m, \;\; m = 1, 2, \ldots, N\}$ is a set of basis functions. The coefficients of the approximate solution q_m are the new unknowns, and equations governing these unknowns are obtained by an integral projection of the governing equations onto the basis set. The weak conservation form is obtained by integrating by parts.

$$
\int_{\Omega} b_k \frac{\partial \mathbf{q}}{\partial t} J \; d\Omega \;\; - \;\; \int_{\Omega} \frac{\partial b_k}{\partial \xi_i} \mathbf{J}^{-1} \mathbf{f}_i J \; d\Omega + \int_{\partial\Omega} b_k (J \mathbf{J}^{-1} \mathbf{f}_i n_i)^R ds = \int_{\Omega} b_k \mathbf{s} J \; d\Omega \tag{3}
$$

for $k = 1, 2, \ldots, N$. Because the solution $\mathbf{q}$ is approximated as a local expansion in terms of the basis functions, both $\mathbf{q}$ and $\mathbf{f}_i$ are discontinuous at the boundaries between neighboring elements. The discontinuity in $\mathbf{q}$ between adjacent elements is treated with an approximate Riemann flux, which is denoted by the superscript R. The Jacobian of the transformation from the global coordinates (x, y) to the local coordinates (ξ, η) of the element is $\mathbf{J}$ and $J = |\mathbf{J}|$. The basis set must be complete, but many classes of functions could be used. A common choice is a set of polynomials of the form $\xi^i \eta^j$ that are defined local to the element. The basis set for degree p contains all polynomials of the form $\xi^i \eta^j$ such that the integers $i + j \leq p$. A possible basis set in two dimensions and $p = 2$ is $\{1, \xi, \eta, \xi^2, \xi\eta, \eta^2\}$.

To implement the quadrature-free approach, the flux $\mathbf{f}_i$ must also be written as an expansion in terms of basis functions:

$$
\mathbf{f}_i(\mathbf{q}) \approx \boldsymbol{f}_{ij}(\mathbf{q}) b_j,
$$

and a similar expansion is made for the approximate Riemann flux and the source $\mathbf{s}$. Because the functional behavior of all of the variables is known, the integrations in equation (3) can be performed analytically. To obtain the values of the integrals for a particular set of coefficients requires the multiplication of a matrix times the vector of the coefficients of the flux polynomial.

The final form of the semi-discrete equation is

$$
\begin{aligned}
\frac{\partial \boldsymbol{q}_m}{\partial t} &= \frac{1}{J}\Big[M_{km}^{-1} A_{ikj} (J \mathbf{J}^{-1} \boldsymbol{f}_{ij}) - M_{km}^{-1} B_{lnk} \left(J \mathbf{J}^{-1} \boldsymbol{f}_{ln} \right)^R \Big] + \boldsymbol{s}_m \\
&= \frac{1}{J}\Big[\tilde{A}_{imj} \tilde{\boldsymbol{f}}_{ij} - \tilde{B}_{lmn} \tilde{\boldsymbol{f}}_{ln}^R \Big] + \boldsymbol{s}_m
\end{aligned} \tag{4}
$$

The exact definitions of the A and B matrices can be found in reference 4. The groupings $\tilde{\boldsymbol{f}}_{ij} = J\mathbf{J}^{-1}\boldsymbol{f}_{ij}$ and $\tilde{\boldsymbol{f}}^R_{ln} = (J\mathbf{J}^{-1}\boldsymbol{f}_{ln})^R$ have been used because that is what is normally stored in the computer implementation. Because all elements of a given type are mapped into the same similarity element, the coefficients $\tilde{A}_{imj}$ and $\tilde{B}_{lmn}$ can be precomputed once and applied throughout the calculation. Equation (4) is advanced in time by using the five-stage, fourth-order, Runge-Kutta method of Kennedy *et al.*[5] Analysis of the stability of this approach can be found in reference 1.

Problem Definition

The DG method was applied to the category 5 problem of the 1999 CAA Workshop on Benchmark problems. The problem involves an acoustic source within a two-dimensional, supersonic shear layer. The velocity profile is given by

$$\overline{U}(y) = \left\{ \begin{array}{l} U_\infty + (U_j - U_\infty)\exp\Big[-(\ln 2)\Big(\frac{y}{b} - \frac{h}{b}\Big)^2\Big],\ y \geq h \\ U_j,\ 0 \leq y < h \end{array} \right\} \tag{5}$$

and the density is obtained from the mean velocity. The mean pressure is uniform, and the flow in the core is at Mach 2. A source term on the pressure equation of the form

$$A\ \exp\Big[-B(\ln 2)(x^2 + y^2)\Big]\cos(\omega t) \tag{6}$$

excites the shear layer with an acoustic source. The parameters are set as follows: $P = 101330$ kg/(m s^2), $h = 0.6$ m, $b = 0.4$ m, $A = 0.001$ kg/(m s^3), $B = 8/\text{m}^2$, T_∞=300 K, and $T_{j0}/T_\infty = 1$. The shear layer is forced at frequencies of St=$2fL/U_j = 0.14$ and 0.6. The length scale $L = 1$ m. The solution is required between $x = 0$ m to 50 m and $y = 0$ m to 10 m.

Solution Procedure

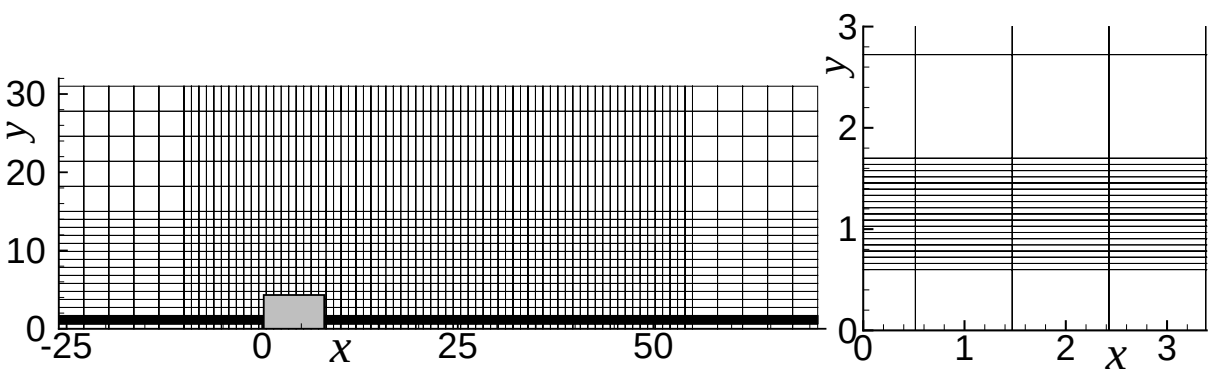

Figure 1: Grid used for the St=0.14 case. Shaded region is enlarged on the right.

A basis set consisting of standard polynomials up to degree four is used which yields a scheme which is fifth-order spatially. The efficient solution procedures discussed in reference 4 about polynomial

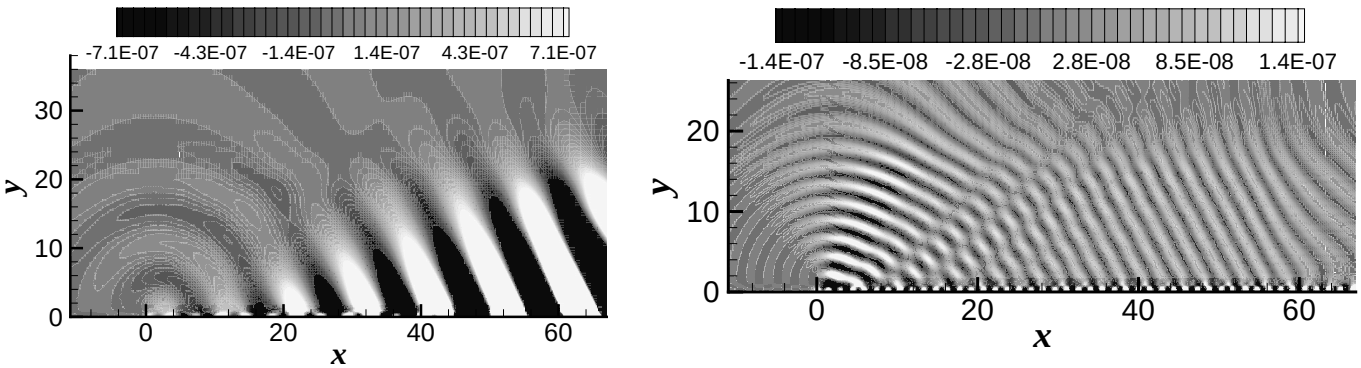

(a) St=0.14 (b) St=0.6

Figure 2: Pressure contours in Pa.

products are used in the current work. A typical grid of rectangular elements is shown in figure 1. The right part of the figure is a magnified view of the grayed out portion of the grid on the left. The enlarged region shows the clustering of elements in the vicinity of the shear layer. Eighteen elements are used between $y = 0.6$ and $y = 1.7$ where $\frac{\partial \overline{U}}{\partial y}$ is large and the perturbation solution varies significantly. Uniform cells are used in the rest of the specified computational domain from x=-5 to 50 and y=0 to 10. A simple symmetry boundary condition is applied along the line $y = 0$. Characteristic conditions[3] on the other boundaries produced unacceptable reflections, so a buffer technique is applied. The region outside of the specified domain is considered the buffer region. The grid spacing is unchanged for 5 m outside of the specified domain extent, then it is abruptly coarsened. Because the DG method is insensitive to grid smoothness, the grid spacing was altered abruptly to conserve grid points without degrading the solution. Within the buffer, the equations are modified to include a Newtonian cooling term,[6] and the mean velocities are modified to obtain supersonic outflow at the boundaries[7] using a $1/2(1 + \cos)$ term. Very little optimization of the buffer parameters was performed. Figure 2 shows the pressure contours throughout the entire computational domain for the two frequencies. The pressure is reported in dimensional units of Pa throughout the paper. A growing instability dominates the low frequency solution, whereas the waves have neutral growth at the higher frequency.

Grid Refinement

A grid refinement was used to assess the quality of the solutions. The number of points within the shear layer was increased first until the growth rate of the instability did not change significantly. Next, the overall number of grid points was varied. Figure 3 shows compares the solutions from two different grids for the St=0.14 case. Figure 3(a) shows the $\overline{p^2}$ along $y = 10$, and (b) depicts the pressure along $y = 1$ at fifty uniformly spaced points between $x = 0$ m and $x = 50$ m. The solutions are very similar for this grid resolution, and the grid can be coarsened considerably with only a small degradation in the solution.

A similar grid refinement for the St=0.6 case is presented in figure 4. Again, the solutions are quite similar between the two grids. Because a fixed number of sampling points are used to generate the figures, the solution looks unresolved in figure 4(b). However, the actual solution is quite smooth.

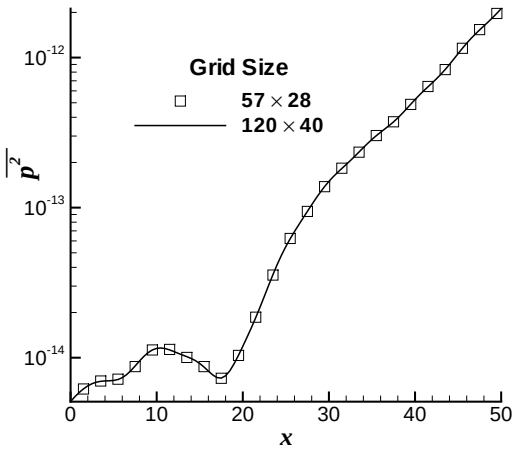

(a) $\overline{p^2}$ along $y = 10$

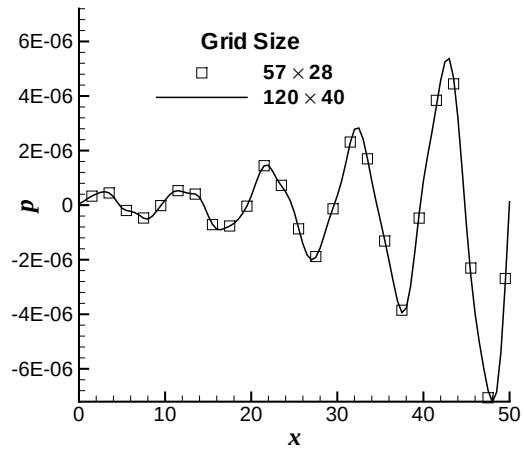

(b) p along $y = 1$

Figure 3: Grid refinement for St=0.14

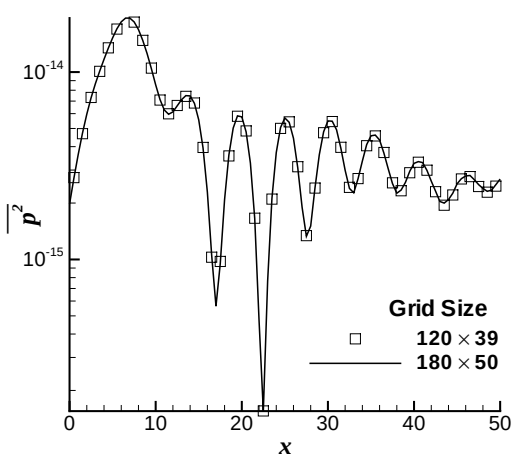

(a) $\overline{p^2}$ along $y = 10$

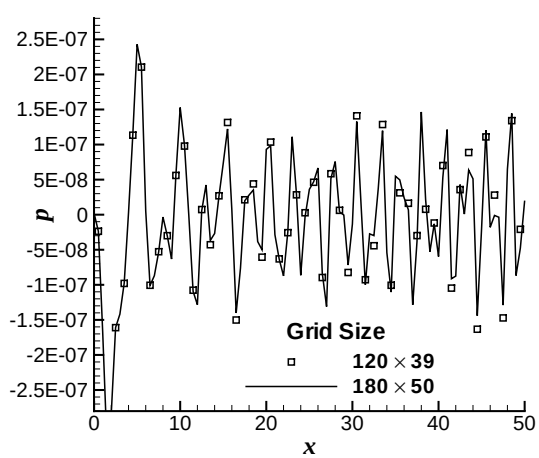

(b) p along $y = 1$

Figure 4: Grid refinement for St=0.6

Buffer Length

Using the coarsest grid that provided a grid independent solution, the length of the buffer was also varied to assess the required length to minimize reflections. Figure 5 reviews the results for the St=0.14 case. The solution along $y = 10$ is more sensitive to the buffer length, but the solutions for the two longest buffer lengths are nearly identical. There is almost no noticeable difference in the solutions along $y = 1$. At the higher frequency, the buffer length was decreased because the wavelength is much shorter. Figure 6 shows that the solutions showed very little variation for the two buffer lengths tested. However, the solution along $x = 50$ m, which is not shown, changed significantly, and a completely grid independent solution was never obtained. The acoustic signal is extremely weak in that region, so even small errors show up in the solution.

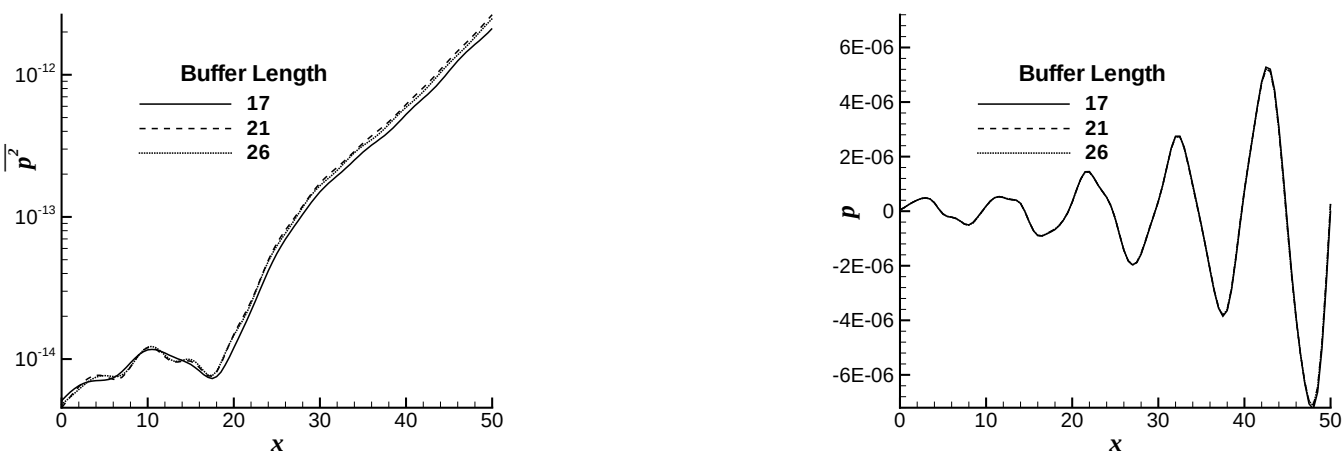

(a) $\overline{p^2}$ along $y = 10$

(b) p along $y = 1$

Figure 5: Variation of solution with buffer length for St=0.14

Resources

This section describes the resources used to obtain the solutions submitted to the workshop. All cases were run on a single processor of a 250 MHz, SGI R10k Octane. There were 3784 fifth-order rectangular elements for the $St = 0.14$ case. The grid was partitioned into several uniformly spaced regions and can be seen in figure 1. Eighteen elements were placed between 0.6 and 1.7 to resolve the shear layer, and 10 elements in the rest of the region up to $y = 10$. The grid was uniform in x with 58 elements between $x = -5$ m and 50 m. The buffer extended an additional 21 m at all inflow/outflow boundaries and required 710 elements. The grid was unaltered in the first 5 m of the buffer, and then the spacing was tripled. 15715 steps were required to run to a time of $t = 15T$ =0.414 s where T is the period of the source. The time step was $\Delta t = 9.54 \times 10^{-4} T$ = 2.635e-5 s. The required CPU time was 5.7 hours.

There were 6816 fifth-order rectangular elements for the $St = 0.6$ case. A refined version of the grid used for the lower frequency was used. Again, eighteen elements were placed between 0.6 and 1.7 to resolve the shear layer, but 24 elements in the rest of the region up to $y = 10$. The grid was uniform in

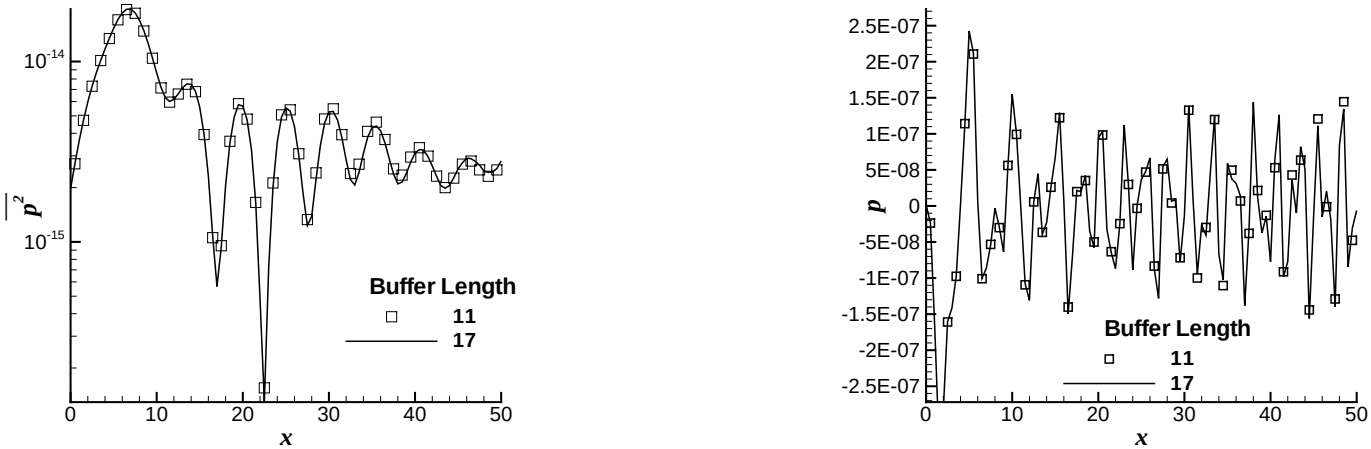

(a) $\overline{p^2}$ along $y = 10$ (b) p along $y = 1$

Figure 6: Variation of solution with buffer length for St=0.6

x with 110 elements between $x = -5$ m and 50 m. The buffer extended an additional 15 m at all inflow/outflow boundaries and required 1226 elements. The grid spacing in the buffer was tripled after 5 m. 13833 steps were required to run to a time of $t = 60T = 0.387$ s where T is the period of the source. The time step was $\Delta t = 4.12 \times 10^{-3} T$ =2.794e-5 s. The required CPU time was 10.2 hours.

References

[1] Atkins, H. L., and Shu, C. W. Quadrature-free implementation of discontinuous Galerkin method for hyperbolic equations. *AIAA Journal*, **36(5)**, pp. 775–782, 1997.

[2] Atkins, H. L. Continued development of the discontinuous Galerkin method for computational aeroacoustic applications. AIAA Paper-97-1581, 1997. Third Joint CEAS/AIAA Aeroacoustics Conference, May 12-14.

[3] Atkins, H. L. Local analysis of shock capturing using discontinuous Galerkin methodology. AIAA Paper 97-2032, 1997. 13th AIAA Computational Fluid Dynamics Conference, Snowmass Village, Colorado, June 29-July 2.

[4] Lockard, D. P., and Atkins, H. L. Efficient implementations of the quadrature-free discontinous galerkin method. AIAA Paper No. 99-3309, July 1999.

[5] Kennedy, C. A., Carpenter, M. H., and Lewis, R. Low-storage explicit Runge-Kutta schemes for the compressible Navier-Stokes equations. to appear in *Applied Numerical Mathematics*.

[6] Israeli, M., and Orszag, S. A. Approximation of radiation boundary conditions. *Journal of Computational Physics*, **35**, pp. 115–135, 1981.

[7] Streett, C. L., and Macaraeg, M. G. Spectral multi-domain for large-scale fluid dynamic simulations. *Applied Numerical Mathematics*, **6**, pp. 123–129, 1989/90.